Vibration of a Translating Roller-Follower Cam with A Preloaded Spring 具預載彈簧的平移式滾子從動件凸輪之振動

Jer-Rong Chang¹ Chun-Jung Huang² Ming-Chih Huang¹ Biing-Hwang Jou¹ Heng-Pin Hsu¹ 張哲榮¹ 黄俊榮² 黄銘智¹ 周炳煌¹ 許恆斌¹

¹Department of Aircraft Engineering, Air Force Institute of Technology

²Department of Aircraft Maintenance, Far East University

1空軍航空技術學院飛機工程系

2 遠東科技大學飛機修護系

Abstract

The aim of this study is to investigate the transverse vibration of a translating roller-follower cam with a preloaded spring. A preloaded spring is set to maintain contact between the roller and the cam throughout the motion cycle. The rise-dwell-fall-dwell (RDFD) motion of the follower is designed by employing the cycloidal displacement. A Rayleigh beam is applied to model the flexible follower. The flexible deformation coupled with the rigid-body translation is considered. The contact position of the roller and the cam is an unknown which cannot be determined only with kinematics analysis. The unknown position will be substituted into the dynamics modeling with considering the geometric constraints. Applying Hamilton's principle with the assumed mode method, the governing equations of motion are derived. The follower vibration responses are obtained using Runge-Kutta method. Then, the influences of system parameters on the vibration of the follower are investigated.

Keywords: spring, cam, roller-follower, translating, vibration

摘要

本研究的目的是檢查預載彈簧的平移式滾子從動件凸輪的側向振動。設置一預載彈簧以保持在運動週期中滾子與凸輪的接觸,從動件的上昇-停滯-下降-停滯運動以擺線輪廓來設計,使用雷利樑模擬撓性從動件,並考慮撓性變形與剛體位移的耦合。滾子與凸輪的接觸點為一未知,無法僅由運動學分析決定。以幾何限制的方式,將此未知位置代入動力模擬。使用漢彌頓原理與假設模態法,導出統御運動方程式。以阮奇-庫達法求解從動件振動響應,並研究系統參數對從動件振動的影響。

關鍵字:彈簧,凸輪,滾子從動件,平移式,振動

1. INTRODUCTION

The kinematics, the dynamics and the design of cam driven mechanisms have been introduced and

discussed extensively[1-2]. Zhou etc. [3] proposed a method for the design and analysis of a high-speed cam mechanism. In the proposed method, the displacement function of the cam follower was

described using Fourier series. A line contact thermo-elasto-hydrodynamics analysis developed by Torabi etc. [4] to study the behavior of the cam and follower contact. The elasto-plastic model took into account the asperity pressure and asperities' flattening due to plastic deformation. The modified Reynolds equation was solved to predict the hydrodynamic pressure. The change in the surface roughness and friction coefficient during the running-in period was taken into account with provision for thermal effects. The results showed performance parameters cam-follower during the running-in period were strongly affected by the rotational speed and thermal effects. It was shown that the rate of flattening of surface roughness is a crucial factor during the running-in period. Chang etc. [5] investigated the transverse vibration of a translating roller-follower cam due to the flexible follower rod under constant rotating speed. The effects of some system parameters on the vibration of the flexible follower have been studied.

In this paper, the transverse vibration of a translating roller-follower cam with a preloaded spring is studied. A preloaded spring is set to maintain the contact between the roller and the cam during the motion cycle. Since the follower is assumed to be flexible, the contact point of the roller and the cam is an unknown though it locates at the cam profile. Lagrange multipliers of two geometric constraints are added to the Hamilton's principle. The assumed mode method is applied to expand the transverse deflection of the follower. The vibration response of the follower is calculated from the derived differential-algebraic equation by applying Runge-Kutta integration method.

2. DERIVATION OF GOVERING EQUATIONS

A translating roller-follower cam with a preloaded spring is shown in Fig. 1. The roller follower consists of a follower rod that has a separate part, the roller, which pinned to the follower stem contacts the rigid cam by using the preloaded spring. The flexible follower rod is modeled as a Rayleigh beam. Following the similar approach of Chang etc. [5], one can derive the system equations of motion to investigate the vibration of the follower with a preloaded spring.

2.1 The kinetic energy and strain energy of the system

Firstly, the kinetic energy and strain energy of

the follower, the strain energy of the preloaded spring, the kinetic energy of the roller, and the work done by the constraint forces are formulated.

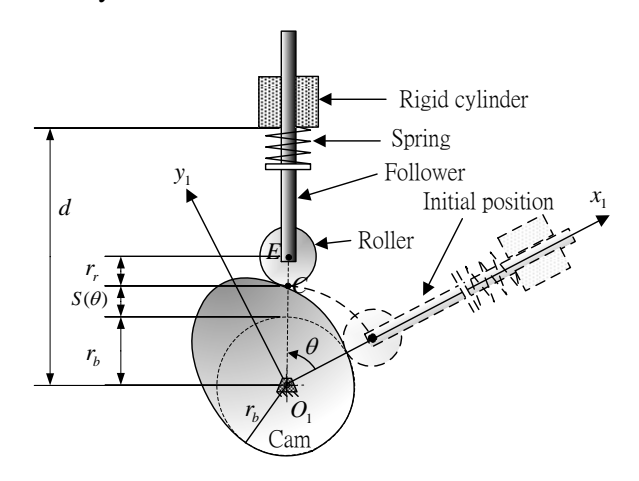


Fig. 1 Schematic of a translating roller-follower cam with a preloaded spring

Figure 1 shows the schematic of a cam mechanism with a preloaded spring. The displacement function of the un-deformed follower rod when the cam rotates with an angle θ is denoted as $S(\theta)$. In Fig. 2, a fixed frame $O_1 - XY$ is used. A rotating frame $O_1 - x_1y_1$ fixed on the cam which rotates with a constant angular speed Ω is applied. A fixed frame $O_2 - xy$ is also used and its unit coordinate vectors are denoted as $\{\mathbf{i}, \mathbf{j}\}^T$. The O_2x axis coincides with the centerline of the un-deformed rod. The flexible follower undergoes a transverse deflection, v(x,t).

The strain energy of the preloaded spring is derived as

$$U_s = \frac{1}{2}k_s(\hat{x} + x_o)^2 \tag{1}$$

where k_s is the preloaded spring stiffness, and $\hat{x} = d - r_b - x_E$. x_E is x coordinate of the end of the follower by using the fixed frame $O_2 - xy$. x_o is the initial amount of compression of the spring. The strain energy U_{rod} of the rod is also derived as follows by applying the strain-stress relationship of Hooke's law,

$$U_{rod} = \frac{1}{2} \int_0^{x_E} E I v_{,xx}^2 dx \tag{2}$$

where E denotes Young's modulus of beam material and I is the area moment of inertia of the rod cross-section.

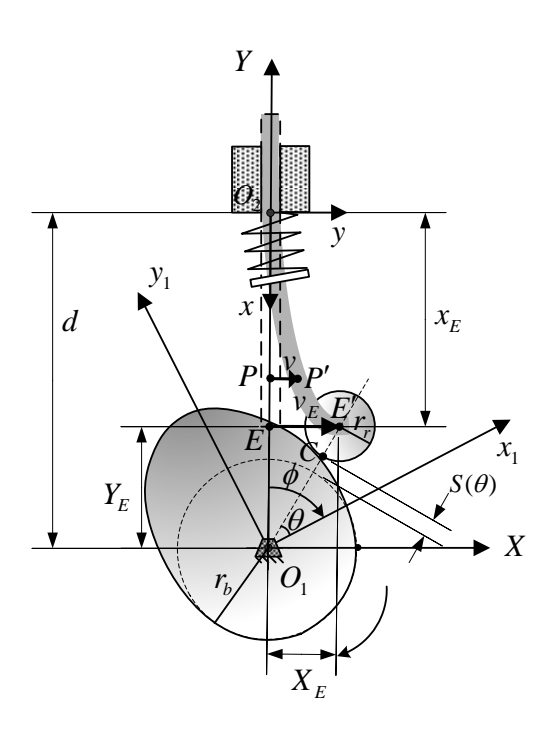


Fig. 2 Deformed configuration of the cam mechanism

The kinetic energy T_{rod} of the rod is expressed as

$$T_{rod} = \frac{1}{2} \int_0^{x_E} \rho A(\dot{x}^2 + \dot{v}^2) dx + \frac{1}{2} \int_0^{x_E} \rho I \dot{v}_{,x}^2 dx$$
 (3)

where ρ , A, and I denotes the mass density, the cross-sectional area, and the cross-sectional area moment of inertia of the rod. The kinetic energy of the roller is derived as

$$T_{roller} = \frac{1}{2} m_r (\dot{X}_E^2 + \dot{Y}_E^2) + \frac{1}{2} \frac{J_r}{r_r^2} [(\dot{X}_C - \dot{X}_E)^2 + (\dot{Y}_C - \dot{Y}_E)^2]$$
(4)

where m_r and J_r are the mass and the polar mass moment of inertia of the roller, respectively. The points C and E are defined in the Fig. 2 and will be derived in the next subsection.

2.2 The constraint equations

The rise-dwell-fall-dwell (RDFD) motion is studied in this paper. The cycloidal displacement is used to describe the cam profile of the rise and the fall motions of the follower. For the rise segment, the displacement function $S(\theta)$ is given as: (Chen [1])

$$0 \le \theta \le \beta : \ S(\theta) = S_T \left[\frac{\theta}{\beta} - \frac{1}{2\pi} \sin(\frac{2\pi\theta}{\beta}) \right] \quad (5)$$

where S_T is the total lift magnitude and β is the period of the rise segment. In this study, β is set to be $\frac{\pi}{2}$. The function in equation (5) is used for the rise portion of the cam. To subtract the rise displacement function $S(\theta)$ from the maximum lift S_T can convert the rise function to the fall function. The period of the fall segment is also set to be $\frac{\pi}{2}$.

Using the theory of envelopes to determine the cam profile, one can derive the profile coordinates (x_{1C}, y_{1C}) as (referring to Fig. 1)

$$x_{1C} = r\cos\theta - \frac{r_r Q}{\sqrt{P^2 + Q^2}},$$

$$y_{1C} = r\sin\theta + (x - r\cos\theta)\frac{P}{Q}.$$
(6)

where r, P, and Q are defined as follows.

$$r = r_b + r_r + S(\theta),$$

$$P = r \sin \theta - S'(\theta) \cos \theta,$$

$$O = r \cos \theta - S'(\theta) \sin \theta.$$
(7)

in which r_b is the base-circle radius of the cam, and r_r is the roller radius. $S'(\theta)$ can be derived by taking derivative of $S(\theta)$, which is listed in Eq. (5), w.r.t. θ .

The $O_1 - x_1 y_1$ coordinates of the roller center E are

$$x_{1E} = r\cos\theta, y_{1E} = r\sin\theta.$$
 (8)

The end point E moves to be E' after deformation. The transverse deflection at the end point E are denoted as v_E , i.e., $v_E = v(x_E, t)$. The fixed coordinates for the points C and E are

$$X_{C} = x_{1C} \sin \Omega t - y_{1C} \cos \Omega t,$$

$$Y_{C} = x_{1C} \cos \Omega t + y_{1C} \sin \Omega t,$$

$$X_{E} = x_{1E} \sin \Omega t - y_{1E} \cos \Omega t,$$

$$Y_{E} = x_{1E} \cos \Omega t + y_{1E} \sin \Omega t.$$
(9)

where Ω is the constant angular speed of the frame $O_1 - x_1 y_1$ fixed on the cam.

Two constraint equations for the point E are derived as follows from the geometric relationship as shown in Fig. 2,

$$\Phi_1 = X_F - \nu_F = 0 \tag{10}$$

$$\Phi_2 = Y_E + x_E - d = 0 \tag{11}$$

2.3 Assumed mode method

For satisfying the boundary condition at the rigid cylinder end, one can expand the deflections by applying assumed mode method as follows,

$$v(x(t),t) = \sum_{i=2}^{N} a_i(t)x(t)^i$$
 (12)

where $x(t)^i$ is the mode shape which is dependent on time since the follower is driven by the cam to lengthen or shorten. It can easily formulate the moving boundary problem though the polynomial expansion is a simple assumed mode method. $a_i(t)$ is the associated amplitude for the transverse deflection.

2.4 Hamilton's principle

Applying Hamilton's principle for the whole system, one has the variation equation as

$$\int_{t_1}^{t_2} \delta(T_{rod} + T_{roller} - U_{rod} - U_s + \lambda_1 \Phi_1 + \lambda_2 \Phi_2) dt = 0$$
(13)

where T_{rod} and T_{roller} are the kinetic energy of the follower rod and the roller, respectively. U_{rod} is the strain energy of the follower rod. U_s is the strain energy of the preloaded spring. $\lambda_1\Phi_1$ and $\lambda_2\Phi_2$ are the works done by the constraint forces.

The system equations of motion are derived by substituting equation (12) into Hamilton's principle (13) and the obtained equations are expressed as

$$\mathbf{M}(\mathbf{Q})\ddot{\mathbf{Q}} + \mathbf{N}(\mathbf{Q}, \dot{\mathbf{Q}}) + \mathbf{\Phi}_{\mathbf{Q}}^{T} \lambda = \mathbf{0}$$
 (14)

where M, N, and λ are mass matrix, nonlinear

vector, and Lagrange multiplier, respectively. M and N are dependent on the mode number in Eq. (12) and thus derived directly by using computer program. Q is the generalized coordinates vector and expressed as

$$\mathbf{Q} = [a_1 \quad a_2 \quad \cdots \quad a_N \quad x_E \quad \theta]. \tag{15}$$

The two constraints in equations (10) and (11) are combined as the following form

$$\mathbf{\Phi}(\mathbf{Q}) = \begin{bmatrix} \Phi_1 & \Phi_2 \end{bmatrix}^T = \mathbf{0} \tag{16}$$

The constraint velocity equations are derived as follows by differentiating equation (16) with respect to time

$$\mathbf{\Phi}_{\mathbf{Q}}\dot{\mathbf{Q}} + \frac{\partial \Phi}{\partial t} = \mathbf{0} \tag{17}$$

The constraint acceleration equations are also derived as follows by differentiating equation (17) with respect to time

$$\mathbf{\Phi}_{\mathbf{Q}}\ddot{\mathbf{Q}} = -\left(\mathbf{\Phi}_{\mathbf{Q}}\dot{\mathbf{Q}}\right)_{\mathbf{Q}}\dot{\mathbf{Q}} - 2\frac{\partial\Phi_{\mathbf{Q}}}{\partial t}\dot{\mathbf{Q}} - \frac{\partial^{2}\Phi}{\partial t^{2}} \equiv \mathbf{\eta} \quad (18)$$

Combining the constraint acceleration equation (18) and the nonlinear ordinary differential equation (14), one obtains the following expression

$$\begin{bmatrix} \mathbf{M} & \mathbf{\Phi}_{\mathbf{Q}}^T \\ \mathbf{\Phi}_{\mathbf{Q}} & \mathbf{0} \end{bmatrix} \begin{bmatrix} \ddot{\mathbf{Q}} \\ \boldsymbol{\lambda} \end{bmatrix} = \begin{bmatrix} -\mathbf{N}(\mathbf{Q}, \dot{\mathbf{Q}}) \\ \boldsymbol{\eta} \end{bmatrix}$$
(19)

The above equations are differential-algebraic equations which govern the vibration of the translating roller-follower cam mechanism with the preloaded spring. Using the partitioning method (Parviz [6]) and Runge-Kutta integration method, one can obtain the dynamic response of the flexible follower with the preloaded spring.

3. NUMERICAL RESULTS AND DISCUSSIONS

To investigate the vibration of the translating roller-follower cam, an example is studied. The stiffness value of the preloaded spring is given as $k_s = 1.32 \times 10^2 \text{ kg/s}^2$. The initial amount of compression of the spring is $x_o = 3.6$ mm. The total lift magnitude S_T for RDFD motion is set to 15 mm. The radius, mass, and mass polar moment of inertia of the roller are $r_r = 5$ mm, and $m_r = 0.05$ kg, respectively. The cross section of the

航空技術學院學報 第十九卷 第9-15頁(民國 109年) Journal of Air Force Institute of Technology, Vol. 19, pp. 9-15, 2020

follower rod makes the lower stiffness of the rod,

and thus induces the larger vibration response.

follower rod is a circle with radius of $r_f = 5 \, \mathrm{mm}$ and the associated cross-sectional area and area inertia are $A = 78.54 \, \mathrm{mm}^2$ and $I = 490.87 \, \mathrm{mm}^4$, respectively. The elastic modulus and the density of the follower rod are $E = 2.1 \times 10^8 \, \mathrm{kg/mm \cdot s^2}$ and $\rho = 7.8 \times 10^{-6} \, \mathrm{kg/mm}^3$, respectively. The base-circle radius of the cam is $r_b = 26 \, \mathrm{mm}$. The distance from the lower end of the rigid cylinder and the rotation center of the cam is $d = 112 \, \mathrm{mm}$.

Zero initial conditions are considered and the time step is set to be $\frac{2\pi}{\Omega} \times 10^{-3}$ s. Three different mode numbers N=2,3,4 are employed to compare the vibration responses for $\Omega=260\,\mathrm{rad/s}$ to check the numerical convergence. The transverse vibration response at the end point E of the follower is shown in Fig. 3. Since the responses curves with N=3 and N=4 are almost coincident, the assumed mode method with N=3 is applied in the following numerical studies.

The transverse responses at the end point E with different spring stiffness coefficient are shown in Fig. 4. The stiffness coefficients of the spring are given as $k_s = 1.32$, 1.32×10^2 , 1.32×10^3 , 3.96×10^3 , 6.60×10^3 kg/s 2 . It is seen that the vibration responses with the stiffness coefficients 1.32, and 1.32×10^2 kg/s 2 are almost coincident. The influences on the follower vibration are significant when the stiffness coefficient is larger than 1.32×10^2 kg/s 2 especially for the rise and the fall segments. The influences are relatively small at the dwell intervals. The high frequency oscillation is found in the dwell interval.

The follower vibrations with three different rotation speeds of cam, $\Omega = 220$, 260, 300 rad/s are analyzed. It is shown from Fig. 5 that the transverse response is larger for the higher cam rotation speed. The vibration response is larger in the rise and the fall segments than that in the dwell segment. However, in the dwell segment, the response is obviously larger for the higher cam rotation speed. It means that the vibration in the dwell segment may not be ignored for the higher cam rotation speed. The vibration responses with three cross-sectional radii of the follower rod, 3.6, 5 and 6.4 mm, are investigated in Fig. 6. It is seen that the vibration responses are larger for the smaller cross-sectional radius of the follower rod. It implies that the smaller cross-sectional radius of The responses of the follower for three different cam base-circle radii, 20, 26, 32 mm, are compared. The results are shown in Fig. 7. It is found that the vibration response is larger for the smaller cam base-circle radius. Under the condition of the same distance d, the follower is relatively longer for the smaller cam base-circle radius and thus the vibration gets larger. Three different total rises, $S_T = 9$, 15 and 21 mm, are also studied. The results

are plotted in Fig. 8. It is seen that the larger total

rise induces the larger vibration response.

4. CONCLUSIONS

The equations of motion for the vibration of a translating roller-follower cam with a preloaded spring for RDFD case are derived by using Hamilton's principle and the assumed mode method. The numerical results for the studied cases show that the influences on the follower vibration are significant when the stiffness coefficient of the preloaded spring is larger than some value especially for the rise and the fall segments. The spring influences are relatively small at the dwell intervals. The vibration response of the follower is larger for the higher rotation speed of cam. In the dwell segment, the response is obviously larger for the higher cam rotation speed. The cases for the follower rod with smaller cross-sectional radius, or the smaller cam base-circle radius, or the larger total rise may induce the larger vibration response amplitude of the follower. Under the analysis of the numerical simulations in this study, the mechanism design for $\Omega = 220 \text{ rad/s}$, $r_f = 6.4 \text{ mm}$, $r_b = 32 \text{ mm}$, $S_T = 9mm$, $k_s = 1.32 \text{ kg/s}^2$, brings about the smaller vibration response amplitude of

REFERENCES

the follower.

- 1. Chen, F. Y., Mechanics and Design of Cam Mechanisms, Pergamon Press, New York, 1982.
- 2. Koloc, Z., and Vaclavik, M., Cam Mechanisms, Elsevier, 1993.
- 3. Zhou, C., Hu, B., Chen, S., and Ma, L., 2016, "Design and analysis of high-speed cam mechanism using Fourier series," Mechanism and Machine Theory, **104**, pp. 118-129.
- 4. Torabi, A., Akbarzadeh, S., Salimpour, M., and Khonsari, M. M., 2018, "On the running-in behavior of cam-follower mechanism," Tribology International, **118**, pp. 301-313.
- 5. Chang, J. R., Huang, M. C., Jou, B. H., and Hsu,

- H. P., 2018, "Transverse vibration analysis of a translating roller-follower cam using cycloidal profile for RDFD motion," Journal of Air Force Institute of Technology, **17**, pp. 115-122.
- 6. Parviz, E. N., Computer-Aided Analysis of Mechanical System, Prentice-Hall International Edition, 1988, pp. 42-46.

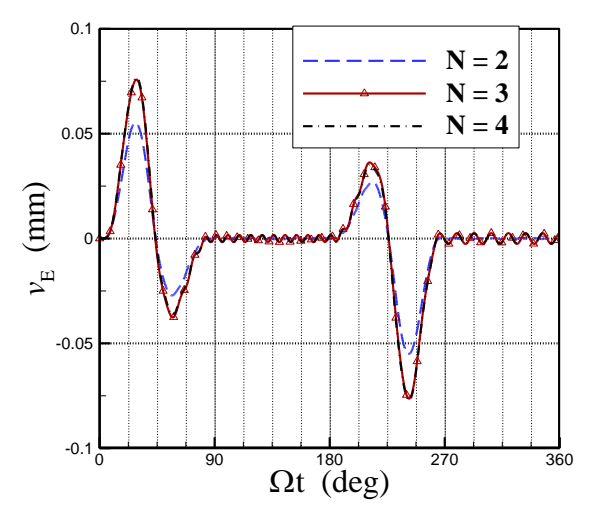


Fig. 3 The transverse vibration response at E with different mode number for $\Omega = 260$ rad/s

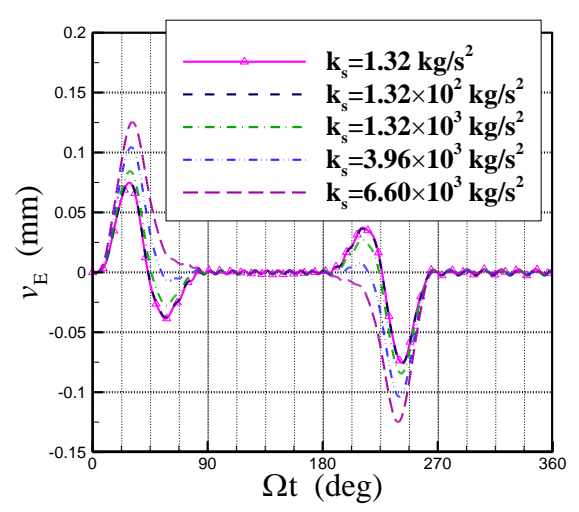


Fig. 4 The transverse vibration response at E with different spring stiffness coefficient k_s

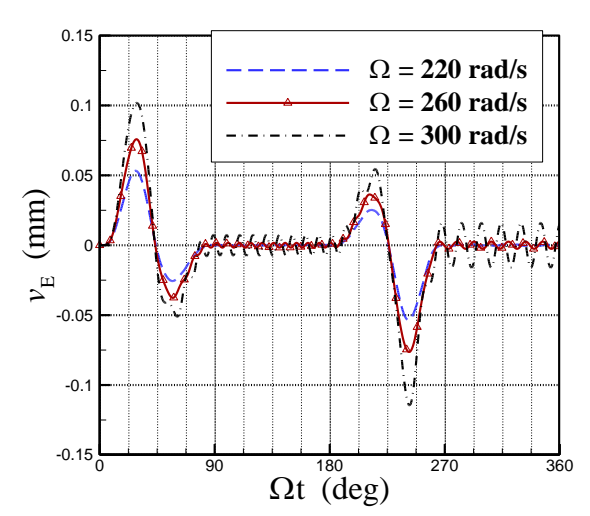


Fig. 5 The transverse vibration response at E with different cam rotation speed Ω

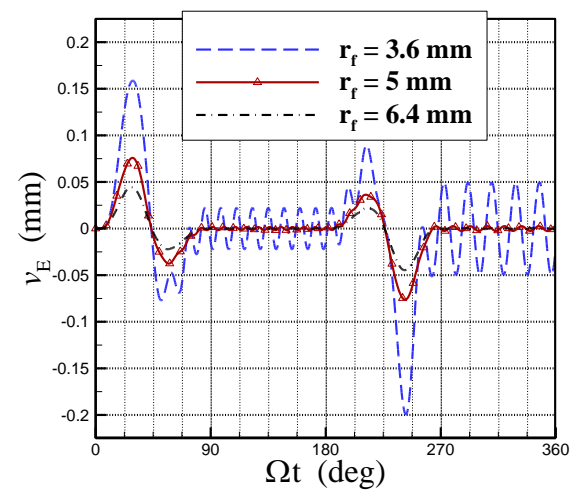


Fig. 6 The transverse vibration response at E with different follower cross-sectional radius r_f

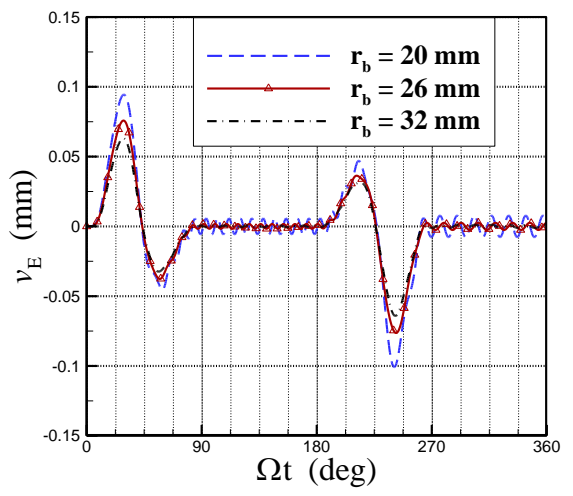


Fig. 7 The transverse vibration response at E with different cam base-circle radius r_b

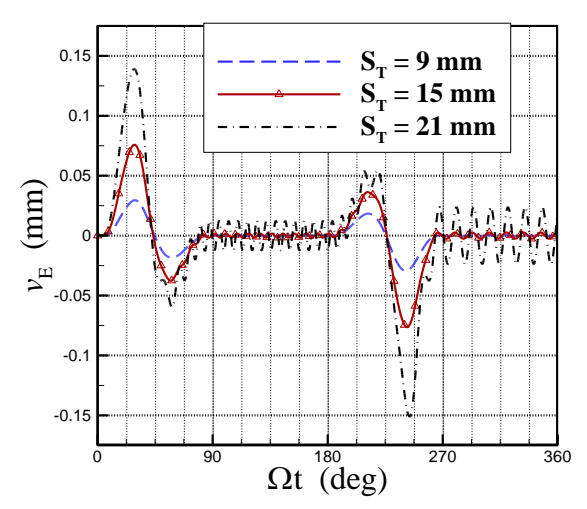


Fig. 8 The transverse vibration response at E with different follower total rise S_T